PROGRESSIVE OPTIMALITY IN HIERARCHICAL FILTER BANKS

Mehmet V. Tazebay and Ali N. Akansu

New Jersey Institute of Technology
Department of Electrical and Computer Engineering
Center for Communications and Signal Processing Research
Newark, NJ 07102

ABSTRACT

The concept of progressive optimization is proposed for the design of hierarchical subband transforms. The time and frequency properties of the product filters in subband trees are discussed and evaluated. It is shown that the performance improvements in image coding are possible by using different PR-QMF banks at different nodes of a subband tree.

I. HIERARCHICAL FILTER BANKS

A generic two-band filter bank structure is given in Fig. 1. It is used as the basic building block of a hierarchical spectral split in this paper because of its historical and practical significance. In general, it is possible to use any number of subbands with the desired bandwidths at any node of a tree.

The hierarchical filter banks in the literature use the same two-band non-ideal prototype filter bank repetitively in the tree without checking the time and frequency properties of the product subband filters. This is a practically significant point and the main topic of this study.

Fig. 2(a) displays a two-stage, 4-band, regular hierarchical subband structure. The two-band filter banks used in the different stages of the tree, even at each node of the same tree level, can be different for the most general subband transform case. Whenever the same prototype filter bank is used in all the nodes, the conventional hierarchical subband tree structure is obtained [1][2].

All of the two-band filter banks employed in the tree are assumed to be PR-QMF in order to satisfy the unitary property of the hierarchical structure.The equivalent subband product filters for the regular tree displayed in Fig. 2 are easily found as

$$\begin{aligned} H_1(z) &= H_0^I(z)H_0^{II}(z^2) \\ H_2(z) &= H_0^I(z)H_1^{II}(z^2) \\ H_3(z) &= H_1^I(z)H_0^{III}(z^2) \\ H_4(z) &= H_1^I(z)H_1^{III}(z^2) \end{aligned} \quad (1)$$

where $H_i(z)$, $i = 1,2,3,4$ are called the product subband filters. The equivalent product filters of the dyadic and irregular subband trees can be similarly obtained.

The time and frequency properties of the second stage filters in Fig. 2(a) are not very critical. But, the properties of the product filters, $H_i(z)$, $i = 1,2,3,4$ along with the first level filters $H_0^I(z)$ and $H_1^I(z)$, are important. Therefore, the intermediary filters of the second stage can be manipulated (since there are infinite possible solutions) in order to achieve the desired time and frequency domain characteristics of the product filters. This leads to the concept of progressive optimization, which will be presented in the next section.

The product subband filters in Eq.(1) are the special 4-band PR-QMF solutions with the factorization properties. They provide the hierarchical as well as the direct split of the spectrum.

Fig. 3 displays the time and frequency functions of two different hierarchical filter bank scenarios. Table 1 provides the time and frequency localizations of the product subband filters of those hierarchical filter banks [3]. Fig. 3 and Table 1 imply the richness of possible product function solutions with the different time-frequency properties in hierarchical filter banks. The design flexibilities of optimal hierarchical subband transforms lead to performance improvements in many signal processing applications such as image coding and spread spectrum communications.

II. PROGRESSIVE OPTIMIZATION IN HIERARCHICAL SUBBAND TRANSFORMS AND A NOTE ON WAVELETS

The progressive optimization of the product subband functions in hierarchical filter banks is proposed

This work was supported in part by GEC-Marconi Corporation

0-8186-6950-0/94 $4.00 © 1994 IEEE

in this section. As an example, let us consider a two-stage 4-band filter bank as displayed in Fig.2. First, an optimal 2-band PR-QMF solution for the first stage is searched based on the defined design criteria. Then an intermediary two-band PR-QMF solution which optimizes the product subband filters is searched. Therefore, the product subband filters of Eq.(1) are tuned to satisfy the desired criteria of optimality, e.g., time localization, frequency localization or joint time-frequency localization. In this study the joint time-frequency spread and energy compaction measures are used separately for the optimal search. The paraunitary condition and the zero-mean high-pass PR-QMF property are forced in the solutions [1].

Fig. 4 displays the frequency functions of the optimal two- and progressively optimal four-band product subband filters. The optimalities in these examples are based on the joint time-frequency localization and energy compaction of the prototype low-pass filter of the two-band PR-QMF [1]. In the two-stage, 4-band, progressively optimal hierarchical PR-QMFs, as seen in Fig. 4(b)-(d), the optimal first stage 2-band 6-tap PR-QMFs are designed. Then in the second stage, 4-tap, 2-band PR-QMF solutions are searched in order to achieve the optimal 12-tap product subband filters based on the design criteria. The detailed treatment of optimal designs is given in [1].

It is seen from this example that the optimal two-band PR-QMF solutions do not yield the optimal product subband filters in hierarchical subband trees. The progressive optimality is a viable approach for the fine tuning of the product subband filter functions. It requires the use of different two-band PR-QMF banks at the different levels, even the different nodes, of the subband tree. Therefore, the practical merits of the optimal wavelet designs based on a prototype two- or M-band optimal discrete-time filter banks are seriously questioned. The infinite resolution products of the discrete-time inter-scale coefficient sequences of the wavelet and scaling bases merge with the analog wavelet and scaling functions in the Fourier domain as [4]

$$\Psi(\Omega) = H_1^I(e^{j\omega/2}) \prod_{k=2}^{\infty} H_0^I(e^{j\omega/2^k}) \quad (2)$$

$$\Phi(\Omega) = \prod_{k=1}^{\infty} H_0^I(e^{j\omega/2^k}) \quad (3)$$

(4)

where $\Psi(\Omega)$ and $\Phi(\Omega)$ are Fourier transforms of the wavelet and scaling functions. The dyadic subband tree can serve as the fast wavelet transform algorithm if the transform process is properly initialized [4][1]. The proper initialization step is the projection of the analog signal onto the scaling space at the full resolution. The sampled data is assumed as the scaling coefficients of the wavelet transform theory in most of the applications reported in the literature. Therefore, they are doing exactly what a discrete-time filter bank does. The wavelet transform on discrete-time signals implies an imperfect representation and it is theoretically incomplete. The decomposition of discrete-time signals is properly realized by the discrete-time subband transforms. The wavelet transform theory will find its meaningful applications in analog signal processing [5].

The proposed progressive optimization in hierarchical filter banks serves as a practical mathematical tool for the design of flexible linear transform bases. The design of irregular spectral decompositions, irregular in the frequency bandwidths as well as in the time domain properties, can be monitored level by level in the subband tree. This approach allows the designer to tune the time and frequency properties of the transform basis to the constraints of the application at hand. The intermediary filters of a given node in the subband tree define the time and frequency properties of the product subband functions for the given optimal filters in the previous level. The repetitive use of an optimal filter bank cell does not yield the optimal product subband functions in a hierarchical structure.

The optimization problem of hierarchical filter banks can also be set in the direct form in order to obtain globally optimal solutions. The direct form with the factorization properties has a much more difficult search procedure than the progressively optimized hierarchical case. The latter breaks the optimization problem into smaller subproblems. Our experience with the available optimization software suggests that the use of the progressive approach is the more viable and better way of solving the problem.

III. EFFECTS OF FILTERS ON HIERARCHICAL SUBBAND IMAGE CODING PERFORMANCE

A dyadic, 10-band, separable 2-D subband transform is employed to test the practical impact of using different filter banks in different levels of the hierarchical structures. The available bits are optimally allocated among the subbands based on their variances. Then, the linear quantizers are employed in the generic subband image codec algorithm. The image coding performance of several hierarchical filter bank scenarios are tested. Fig. 5 displays the rate-distortion curves of different 10-band 2-D subband codecs for the test images, LENA and BUILDING. These figures also indicate the filters employed in the considered hierarchical

subband coding experiment. The first index implies the filter used in the first level of the subband tree and the others follow similarly. The known PR-QMF families in the literature are used in these experiments. It is observed from the figures that the different image coding performances are obtained with different subband filter banks. This result is due to different time-frequency properties of the product subband functions of filter banks employed in the coding experiments. More experimental studies to find the best possible filter bank configurations for certain image families are topics of future research. Future studies should also focus on the subjective coding performance of the subband transform bases.

IV. CONCLUSIONS

The hybrid subband/DCT image coding algorithm proposed in Ref. [6] implicitly use the proposed idea in this paper. The performance and design issues of hierarchical filter banks are addressed. A novel, progressively optimal design technique for the hierarchical filter banks is proposed. The significance of the proposed approach in the design of flexible linear transform bases is discussed. The practical assessment of using different filter banks at different nodes of a subband tree is made with some image coding experiments. The image compression performance of several filter bank configurations are shown to be different, as expected. It is observed from the coding experiments that the performance improvements are possible. The other applications of linear transforms will also benefit from the proposed idea.

References

[1] A.N. Akansu, and R.A. Haddad, *Multiresolution Signal Decomposition: Transforms, Subbands, and Wavelets.* Academic Press Inc., 1992.

[2] P.P. Vaidyanathan, *Multirate Systems and Filter-banks.* Prentice Hall, 1993.

[3] R.A. Haddad, A.N. Akansu, and A. Benyassine, "Time-Frequency Localization In Transforms, Subbands And Wavelets: A Critical Review," Optical Engineering, pp. 1411-1429, Vol. 32, July 1993.

[4] I. Daubechies, "Orthonormal Bases of Compactly Supported Wavelets," Comm. in Pure and Applied Math., vol. 41, pp. 909-996, 1988.

[5] R.T. Edwards and M.D. Godfrey, "An Analog Wavelet Chip for Speech Compression," Chip Specifications, ZILOG Inc., Dec. 3, 1992.

[6] R. Ansari, A. Fernandez and S.H. Lee, HDTV Subband/DCT Coding Using IIR Filter Banks: Coding Strategies, Proc. SPIE Conference on Visual Communications and Image Processing, Philadelphia, PA, Vol. 1199, pp. 1291-1302, Nov. 1989.

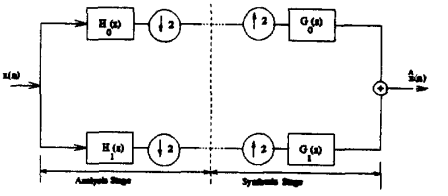

Figure 1: 2-band Filter Bank

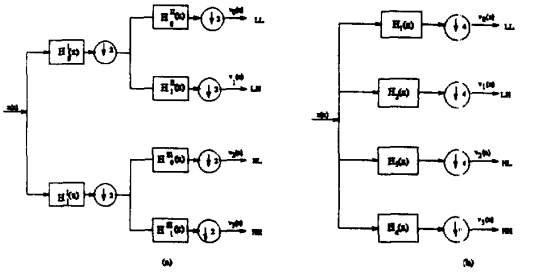

Figure 2: (a) 2-stage, 4-band hierarchical filter bank; (b) the equivalent direct form 4-band filter bank

Table 1: Time and frequency localizations of hierarchical filter banks displayed in Fig. 3 and Fig. 4.

	$\bar{\omega}$	$\bar{n}$	σ_ω^2	σ_n^2	$\sigma_\omega^2 \times \sigma_n^2$
B-QMF Hierarchical 4-band Tree (22 tap product filters)	0	4.05	0.2526	2.7261	0.6886
	1.23	12.88	0.1222	3.8269	0.4676
	1.91	16.28	0.1222	2.7757	0.3392
	π	8.80	0.2526	2.2622	0.5714
Hierarchical 4-Band Tree; 4-tap B-QMF at the first stage, 16-tap B-QMF at the low and 4-tap B-QMF at the high-pass nodes of the second stage	0	4.5535	0.2857	9.8246	2.8072
	1.31	27.1486	0.1447	10.1603	1.4712
	1.88	6.3267	0.1718	1.7254	0.2964
	π	3.9722	0.3697	1.4089	0.5210
Progressively optimized 4-band tree, 12-tap product filters. (Optimality is based on minimization of joint time-frequency spread of the filters)	0	1.8696	0.3562	1.1751	0.4186
	1.20	5.8878	0.1623	1.6811	0.2730
	1.94	8.8042	0.1623	1.6811	0.2730
	π	5.4382	0.3562	1.1751	0.4186
Progressively optimized 4-band tree, 12-tap product filters. (Optimality is based on the energy compaction measure)	0	2.5664	0.2910	1.5319	0.4458
	1.21	5.6715	0.1385	2.2932	0.3177
	1.93	7.9264	0.1385	1.9780	0.2740
	π	5.8354	0.2910	1.3592	0.3955

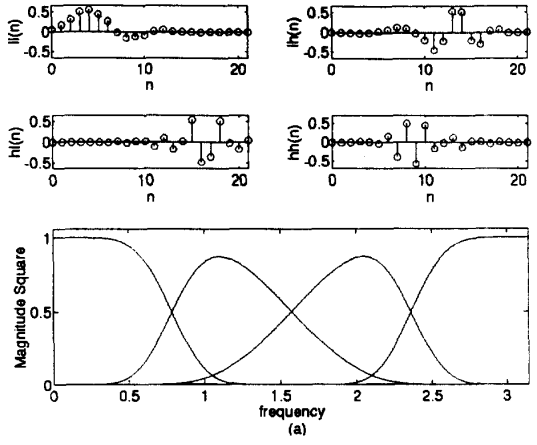

Figure 3: (a) Time and frequency functions of the product subband filters in a 2-level, 4-band hierarchical filter bank using an 8-tap Binomial QMF-Wavelet Filter Bank [1][4] repetitively at any node of the tree.

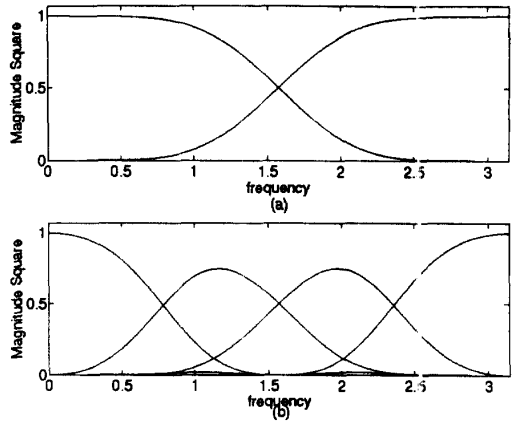

Figure 4 : The frequency functions of (a) 6-tap optimal 2-band PR-QMF. Optimality is based on the minimization of the joint time-frequency spread. (b) 12-tap product subband filters of progressively optimal 4-band PR-QMF. The optimality is based on the progressive optimization of the product filters with the minimization of the joint time-frequency spread.

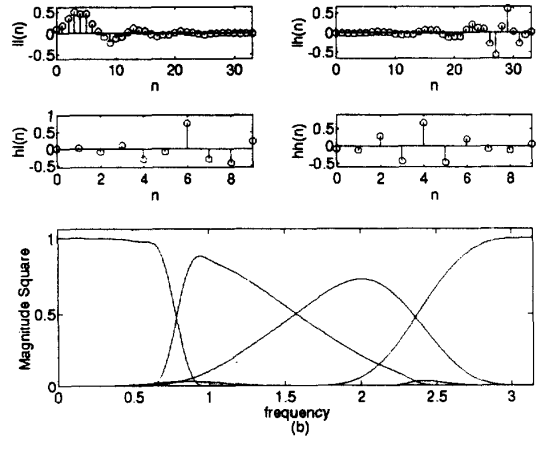

Figure 3: (b) Time and frequency functions of the product subband filters in a 2-level, 4-band hierarchical filter bank using 4-tap Binomial QMF-Wavelet Filter Bank [1][4] at the first stage, 16-tap version at the low, and 4-tap version at the high-pass node of the second stage.

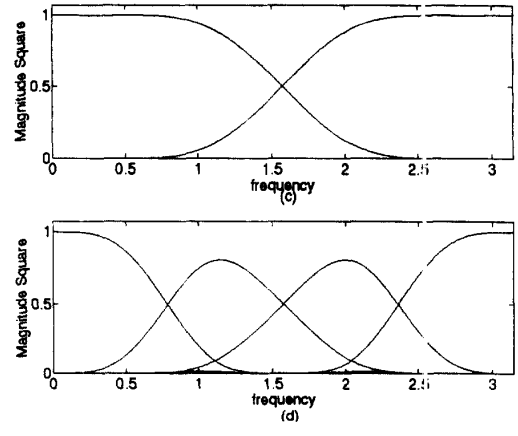

Figure 4 : (c) 6-tap optimal 2-band PR-QMF. Optimality is based on the energy compaction measure. (d) 12-tap product subband filters of progressively optimal 4-band PR-QMF. The optimality is based on the progressive optimization of the product filters with the energy compaction measure.

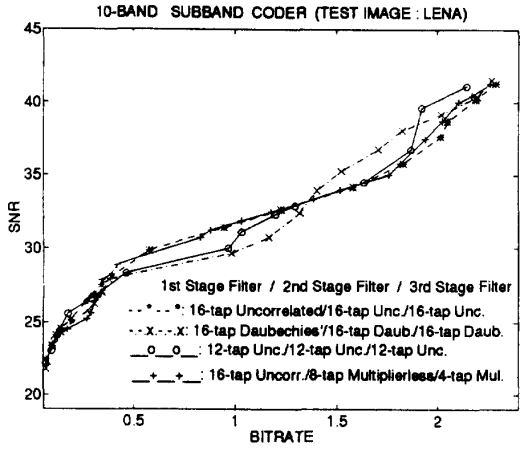

Fig. 5 :(a) Rate-distortion curves of different filter combinations for the test image LENA

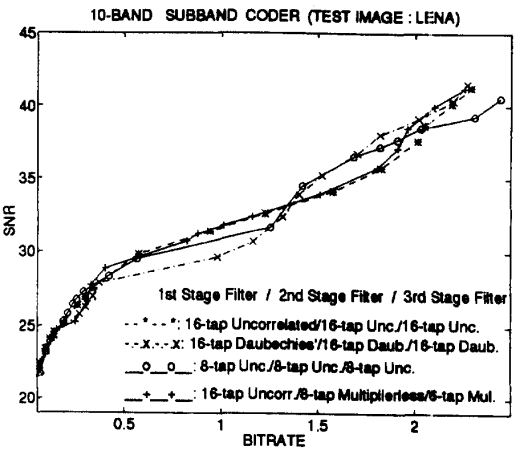

Fig. 5 :(b) Rate-distortion curves of different filter combinations for the test image LENA

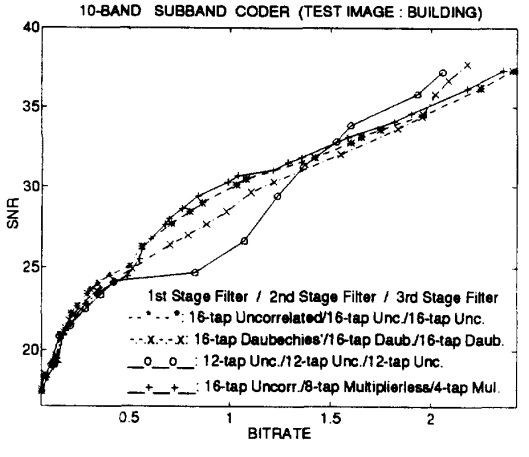

Fig. 5 :(c) Rate-distortion curves of different filter combinations for the test image BUILDING

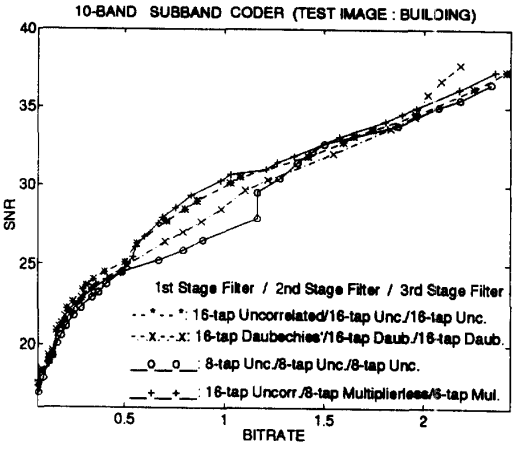

Fig. 5 :(d) Rate-distortion curves of different filter combinations for the test image BUILDING